Coexistence of Large Thermopower and Degenerate Doping in the Nanostructured Material $Ag_{0.85}SnSb_{1.15}Te_3$

John Androulakis,[†] Robert Pcionek,[†] Eric Quarez,[†] Jun-Huang Do,[†] Huijun Kong,[‡] Oleg Palchik,[‡] C. Uher,[‡] Jonathan James D'Angelo,[§] Jarrod Short,[§] Tim Hogan,[§] and Mercouri G. Kanatzidis*,[†]

Department of Chemistry and Electrical and Computer Engineering Department, Michigan State University, East Lansing, Michigan 48824, and Department of Physics, University of Michigan, Ann Arbor, Michigan 48109

Received May 16, 2006
Revised Manuscript Received July 17, 2006

Thermoelectric materials are currently the subject of considerable scientific and technological interest as they promise applications for direct heat to electric power generation and cooling yet present a formidable challenge of raising their performance.[1] The relation $ZT = (S^2\sigma/\kappa)T$, is called the dimensionless figure of merit, where σ is the electrical conductivity, S is the thermoelectric power or Seebeck coefficient, and κ is the thermal conductivity, and is used to evaluate the efficiency of a material. The physical interdependence of σ, S, and κ has historically hindered the identification of high performance materials. The best compromise is realized for a heavily doped semiconductor ($\sim 10^{19}$ carriers/cm^3), where further improvement is possible through tuning the lattice part of the thermal conductivity. Invariably, when the doping exceeds 10^{20} carriers/cm^3 it leads to very small $S < 60$ μV/K.[1]

Here we report on $Ag_{1-x}SnSb_{1+x}Te_3$, an interesting material system with a surprising combination of electrical properties. This compound is a non-stoichiometric derivative of $AgSnSbTe_3$ which is formed from the combination of two isotypic narrow band gap semiconductors, $AgSbTe_2$ and SnTe, both of which adopt the NaCl structure.[2] To the best of our knowledge $Ag_{1-x}SnSb_{1+x}Te_3$ exhibits an exceptional combination of large thermoelectric power response of ~160 μV/K and a heavy carrier mass despite an enormous almost metallic carrier concentration ($\sim 5 \times 10^{21}$ carriers/cm^3). This is unique behavior and is not found in the parent $AgSbTe_2$[2,3] and SnTe[4] compounds. The origin of this outstanding physical response could lie in the fact that $Ag_{1-x}SnSb_{1+x}Te_3$ is actually ordered on two length scales. It exhibits local atomic ordering as well as nanostructuring associated with compositional fluctuations on the 2−5 nm scale.

$AgSnSbTe_3$ samples were produced by mixing appropriate stoichiometric ratios of high purity Ag, Sn, Sb, and Te. The initial charge was sealed in evacuated fused silica tubes, heated at 1000 °C, held there for 4 days, and then slowly cooled to room temperature. All data presented in this paper were obtained on the same crystal batch. Samples were characterized using powder and single-crystal X-ray diffraction (described in Supporting Information), scanning electron microscopy coupled with analysis by an energy dispersive X-ray spectrometer and high-resolution field emission transmission electron microscope (JEOL-2200FS) attached to a Gatan image filter. Details regarding the experimental apparatus used to determine the thermal and charge transport properties can be found elsewhere.[5,6]

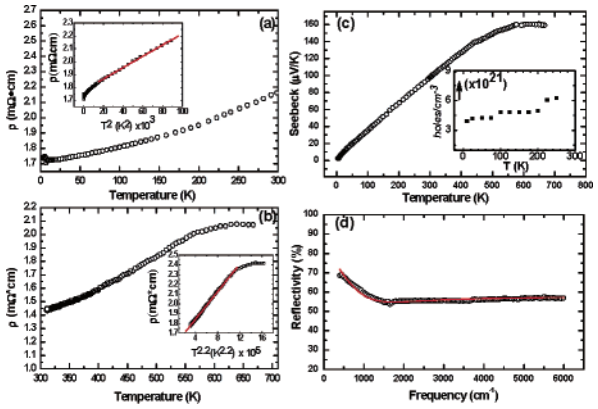

Figure 1. (a) Electrical resistivity of $Ag_{0.85}SnSb_{1.15}Te_3$ in the temperature range $4.2 \leq T \leq 300$ K. (b) Resistivity in the range $300 \leq T \leq 700$ K. Insets depict fits to T^n law dependence ($n = 2, 2.2$). (c) Temperature dependence of the Seebeck coefficient. Inset: hole concentration as a function of temperature. (d) Room-temperature optical conductivity (open circles) in the frequency range 400−6000 cm^{-1} analyzed with the Drude model (solid line).

Figure 1a,b shows the behavior of the resistivity at low and high temperatures. The resistivity steadily increases with increasing temperature, a fact consistent with the doping level of the sample that renders it almost metallic. Starting around 550 K the $\rho(T)$ curve changes slope forming a plateau which persists up to the highest temperature of the measurement. Below 550 K an almost quadratic power law dependence of the resistivity, $\rho(T) \sim T^{2.2}$, which persists down to room temperature, was observed. The same is true for the low-temperature data set in the range $160 \leq T \leq 300$ K where quadratic behavior is observed [$\rho(T) \sim T^2$]; see Figure 1, insets. Although a T^2 scaling normally pertains to electron−electron interactions, this may not be the mechanism at such elevated temperatures where electron−phonon scattering can dominate and eventually mask all other interactions.[7,8]

The Hall voltage was positive, and the Hall coefficient was linear in field up to the highest magnetic field measured ($H_{max} = 5T$) and at all temperatures, indicating, therefore,

[†] Department of Chemistry, Michigan State University.
[‡] University of Michigan.
[§] Electrical and Computer Engineering Department, Michigan State University.

(1) Slack, G. A. In *CRC Handbook of Thermoelectrics*; Rowe, D. M., Ed.; CRC Press: Boca Raton, 1995.
(2) Rosi, F. D.; Hockings, E. F.; Lindenblad, N. E. *RCA Rev.* **1961**, *22*, 82. Ono, T.; Irie T.; Taahama, T. *J. Phys. Soc. Jpn.* **1962**, *17*, 1070. Ishihara, T. *J. Phys. Soc. Jpn.* **1962**, *17*, 719.
(3) Armstrong, R. W.; Faust, J. W., Jr.; Tiller, W. A. *J. Appl. Phys.* **1960**, *31*, 1954.
(4) Damon, D. H. *J. Appl. Phys.* **1966**, *37*, 3181.
(5) Chung D. Y.; Hogan, T. P.; Rocci-Lane, M.; Brazis, P.; Ireland, J. R.; Kannerwurf, C. R.; Bastea, M.; Uher, C.; Kanatzidis M. G. *J. Am. Chem. Soc.* **2004**, *126*, 6414.
(6) Loo, S.; Short, J.; Hsu, K.-F.; Kanatzidis, M. G.; Hogan, T. *MRS Symp. Proc.* **2004**, *793*, 375.
(7) Yonezawa, S.; Maeno, Y. *Phys. Rev. B* **2003**, *70*, 184523 and references therein.
(8) Tokura, Y.; Taguchi, Y.; Okada, Y.; Fujishima, Y.; Arima, T.; Kumagai, K.; Iye, Y. *Phys. Rev. Lett.* **1993**, *70*, 2126.

10.1021/cm061151p CCC: $33.50
Published on Web 09/01/2006

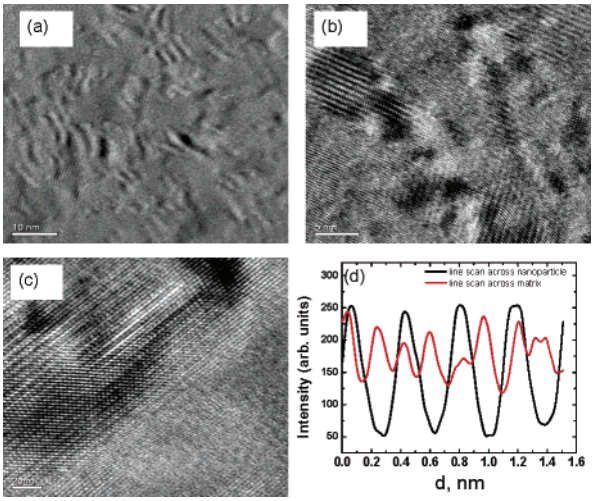

Figure 2. (a) High-resolution TEM image of $Ag_{0.85}SnSb_{1.15}Te_3$ which shows a nanostructured region of the crystal. The nanostructures have geometrical dimensions of 3−30 nm and are dispersed throughout the crystal evenly (scale bar (sb) 10 nm). (b) A close-up view of an embedded nanocrystal (sb 5 nm). (c) The interface region between the embedded nanocrystal and the matrix showing a high degree of coherency (sb 2 nm). (d) Line scan across the nanoparticle (left side) of Figure 2c and matrix (right side) showing the doubling of the periodicity in the former.

p-type conduction. The measured carrier concentration is of the order of 10^{21} carriers/cm^3 assuming one carrier type and parabolic bands in our analysis, Figure 1a,c. This highly degenerate (almost metallic) compound has a carrier concentration that approaches stoichiometric levels at an average of 0.3 carriers/f.u., which is approximately the deviation of the $Ag_{1-x}SnSb_{1+x}Te_3$ formula from its ideal (i.e., $x = 0$). Under these conditions, it is surprising to observe such large values of thermopower (vide infra).

The thermopower of the compound as a function of temperature is plotted in Figure 1c. The data from the low temperature apparatus (5−300 K) were consistent with those at high temperatures (300−650 K). The absolute value of the thermopower is positive, indicating p-type conduction, in agreement with the Hall effect results, and rises linearly from very small values (<5 μV/K) at 4.2 K to 165 μV/K at 650 K. Certainly, such a large thermopower is very unusual for a highly degenerate semiconductor. At higher temperatures the curve bends to lower values indicative of the onset of intrinsic conduction, thereby reducing the absolute thermopower. This thermoelectric response is also in agreement with the resistivity plateau at ∼600 K described above.

A high thermoelectric power has been reported in the rare-earth intermetallics $YbAl_3$ (−80 V/K at 200 K) and $CePd_3$ (120 μV/K at 125 K).[9,10] The underlying reason in these metallic systems, however, has more to do with mixed rare earth element valency and the associated magnetism. For $YbAl_3$ and $CePd_3$, the thermopower peak appears at low temperatures (80−150 K) and is followed by a monotonic decrease at higher temperatures. For $Ag_{0.85}SnSb_{1.15}Te_3$ the thermopower increases linearly up to 600 K, reaching a maximum of ∼165 μV/K. We believe this is the first report of a thermopower of this magnitude in such a heavily doped system (containing no magnetic elements) at high temperature. This observation implies that classes of materials could exist that depart from the conventional behavior of interdependence between high carrier concentration and low thermopower which certainly warrants further investigations.

The concomitant very high thermoelectric response and extremely high carrier concentration can be reconciled through a heavy hole effective mass, m^*. A direct approach to estimate the effective mass is to analyze the infrared reflectivity within the context of the one band Drude model.[11] Figure 1d shows the room-temperature reflectivity of the compound in the range 400−6000 cm^{-1}. The plasma frequency, ω_p, deduced from the fit in conjunction with the results of Hall effect measurements on the carrier concentration were used to determine m^* using the formula

$$\omega_p = \frac{pe^2}{m^*\epsilon\epsilon_\infty}$$

where ϵ_∞ is the high-frequency dielectric constant of the sample and ϵ is the permittivity of free space. This yields an effective mass of $\sim 6m_0$ for a room-temperature carrier concentration of $p = 6.2 \times 10^{21}$ carriers/cm^3.[12] A relatively heavy electron effective mass on the order of $\sim 3m_0$, which yields high thermopower, has been observed in the Half-Heusler compound ZrNiSn; however, the carrier concentration is 1 to 2 orders of magnitude lower.[13a] Furthermore, some n-type skutterudite compounds have been reported to exhibit high carrier densities (∼10^{21} carriers/cm^3) and a high effective mass (∼5−6m_0), but the high temperature thermopower of these systems does not exceed 100 μV/K.[13b] For comparison, the hole effective mass of the more chemically related PbTe is 0.215, for PbSe it is 0.18,[1] and for SnTe it is ∼0.1.[14] Therefore, the physical origin of the massive hole in $Ag_{0.85}SnSb_{1.15}Te_3$ is an open scientific issue. If proper models can be constructed for this material, new insights might be obtained through electronic band structure calculations. The widely dispersed nanostructuring in this material (see below) compared to that in $AgSbTe_2$ and SnTe may also be responsible for this unusual behavior.

Another interesting feature of $Ag_{1-x}SnSb_{1+x}Te_3$ is that its p-type charge transport is opposite to what would be expected. Excess Sb atoms in the structure should generally act as electron donors. This coupled with the deficiency of Ag atoms which act as acceptors should lead to n-type behavior, but this clearly is not observed.

Min and Rowe have expressed the thermopower of a semiconductor in terms of the simple formula $S = m(b - \ln \sigma)$, where $m = k_B/e$ and σ is the electrical conductivity.[15]

(9) (a) Gambino, R. J.; Grobman, W. D.; Toxen, A. M. *Appl. Phys. Lett.* **1973**, *22*, 506. (b) Proctor, K. J.; Jones, C. D. W.; DiSalvo, F. J. *J. Phys. Chem. Solids* **1999**, *60*, 663−671.
(10) Rowe, D. M.; Kuznetsov, V. L.; Kuznestsova, L. A.; Min, G. *J. Phys. D: Appl. Phys.* **2002**, *35*, 2183.
(11) Kittel, C. In *Introduction to Solid State Physics*, 5th ed.; John Wiley & Sons: New York, 1976; p 323.
(12) The fit yields an effective mass of $\sim 6m_0$. The physical parameters corresponding to the one band model fit are $\omega_p \sim 1200$ cm^{-1}, $\epsilon_\infty \sim 65$, and the inverse scattering time, $\Gamma \sim 1600$ s^{-1}.
(13) (a) Uher, C.; Yang, J.; Hu, S.; Morelli, D. T.; Meisner, G. P. *Phys. Rev. B* **1999**, *59*, 8615. (b) Uher, C. *Semicond. Semimet.* **2001**, *69*, 139.
(14) Savage, H. T.; Houston, B.; Burke, J. R., Jr. *Phys. Rev. B* **1972**, *6*, 2292.
(15) Min, G.; Rowe, D. M. *Appl. Phys. Lett.* **2000**, *77*, 860.

The parameter b depends on the temperature, carrier mobility, and carrier effective mass as follows:

$$b = s + \ln[T^{3/2}(m^*/m_0)^{3/2}\mu]$$

where s is a constant associated with the carrier scattering mechanisms, m^* is the effective mass, m_0 is the free electron mass, and μ is the carrier mobility. We are not aware of any semiconductors for which $b \geq 10$.[15] On the basis of the aforementioned results on $Ag_{0.85}SnSb_{1.15}Te_3$ we calculate that $b \geq 11$. This suggests that the underlying scattering physical mechanisms may be much more complex than those assumed by Min and Rowe or that a simple semiconductor model may not be appropriate to describe these novel systems.

Single-crystal X-ray data refinements on specimens selected from ingots of $Ag_{0.85}SnSb_{1.15}Te_3$ are consistent with either the $Pm\bar{3}m$ or the $P4/mmm$ space group as reported for similar compounds.[16] In the tetragonal model, the cations separate into alternating layers of Ag/Sb and Sn atoms stacked along the c axis (Figure 3S in Supporting Information). The NaCl-type $Fm\bar{3}m$ space group (indicated by X-ray diffraction) was ruled out because it did not account for ~40% of the observed reflections. In the $Pm\bar{3}m$ model the Na-site of the $Fm\bar{3}m$ structure splits into two unique sites which accommodate some ordering of Ag, Sn, and Sb atoms. The single-crystal studies which indicate atomic ordering and lower symmetry still represent an averaged structure. Therefore, we probed the material on the nanoscale with high-resolution transmission electron microscopy (TEM), which revealed surprising and unanticipated features.

High-resolution microscopy study of $Ag_{0.85}SnSb_{1.15}Te_3$ indicates that the system is a nanostructured composite rather than a solid solution (see Figure 2a). The pattern shown in Figure 2a is repeated throughout the crystal specimen under observation thereby creating a dense nanostructured system, a type of "bulk nanocomposite". A closer view of the nanoregions (Figure 2b) show that their structural arrangement is considerably altered from the matrix surrounding them because a doubling of the cell can be observed. Line scans inside and outside of the nanoregions reveal the appearance of a superstructure, Figure 2c. Furthermore, as Figure 2a,c shows the nanoregions are coherently embedded in the matrix, they thus do not disrupt the surrounding atomic order which could potentially lead to electron scattering. These distinct compositional fluctuations at the nanoscopic level have striking similarities to those of $AgPb_mSbTe_{m+2}$.[17]

We have tried unsuccessfully to produce an actual solid solution by quenching samples from 575 °C (the melting point of the compound is ~607 °C). Also, long term heating below the melting point did not change the presence of nanostructures. This suggests that the $AgSbTe_2-SnTe$ system has a strong tendency toward the formation of this type of nanophase separation. Therefore, it seems reasonable to conclude that this attribute is thermodynamically stable and could lie at the heart of the explanation of the observed physical properties.

The lattice thermal conductivity of $Ag_{0.85}SnSn_{1.15}Te_3$ is very low and nearly constant from 100 to 300 K ~0.9 W/m·K (Figure 1S, Supporting Information). The surprisingly low value of κ_{lat} (0.9 W/m·K) is similar to that of $AgSbTe_2$ and does not seem to be highly affected by the introduction of SnTe. In previous studies the relative insensitivity of the thermal conductivity of $AgSbTe_2$ upon alloying with SnTe was attributed to the existence of complete solid miscibility in the system.[2] On the basis of our TEM results, however, complete miscibility does not seem to be the case. We suggest that the nanostructures efficiently scatter phonons in the materials which results in the very low thermal conductivity.

Rosi et al. have emphasized that the principal drawback that precludes $AgSbTe_2$ from being used in power generation applications at intermediate temperatures is the inability to controllably dope it to a resistivity below 2 mΩ·cm.[2] Our work suggests $Ag_{1-x}SnSb_{1+x}Te_3$ as a very interesting alternative to $AgSbTe_2$ without compromising its most desirable properties, which are the low thermal conductivity and concurrent high thermoelectric power.

In conclusion, $Ag_{1-x}SnSb_{1+x}Te_3$ presents a unique combination of a large positive thermoelectric power response (although expected negative) of ~160 μV/K with an almost metallic carrier concentration (~5×10^{21} carriers/cm^3). This peculiar state arises from a high effective mass for the hole carriers. Such observations highlight the challenges that remain in understanding the physical properties of chalcogenide-based materials even after decades of research. $Ag_{0.85}SnSb_{1.15}Te_3$ is a bulk nanostructured material and not a solid solution (also known as spinodal decomposition). The development of distinct nanostructuring arises from thermodynamically driven compositional fluctuations. This leads to a very low thermal conductivity, which is in accord with recent results on thermal transport in heterogeneous systems.[18]

Acknowledgment. The authors thank Prof. S. D. Mahanti for useful discussions. Financial support was provided from the Office of Naval Research (N00014-02-1-0867 MURI program).

Supporting Information Available: Synthesis, powder X-ray diffraction, scanning electron microscopy, single-crystal X-ray diffraction, energy-dispersive X-ray analysis, crystal structure refinements, atomic parameters and isotropic displacement parameters, graphical representations of the crystal structures, thermal conductivity, and thermoelectric figure of merit (PDF, CIF). This material is available free of charge via the Internet at http://pubs.acs.org.

CM061151P

(16) The refinements were straightforward and were carried out as detailed in ref 17. The tetragonal model gave better refinement results than the cubic one when considering all data. Single crystal refinement details are as follows. Cubic model: $a = 6.1731(5)$ Å, $Pm\bar{3}m$ space group (86 unique reflections; $R_{int} = 2.85\%$; no. of refined parameters, 6; R_1/wR_2 for all data, 2.73%/3.82%). Tetragonal model: $a = 4.3650(5)$ Å, $c = 6.1731(5)$ Å, $P4/mmm$ space group (112 unique reflections; $R_{int} = 2.31\%$; no. of refined parameters, 6; R_1/wR_2 for all data, 2.09%/3.70%). The formula obtained after refinement was $Ag_{1.33}Sn_{1.33}Sb_{1.33}Te_4$ which corresponds to $AgSnSbTe_3$ ($m = 1$) in the formula scheme of $AgSn_mSbTe_{m+2}$.

(17) Quarez, E.; Hsu, K.-F.; Pcionek, R.; Frangis, N.; Polychroniadis, E. K.; Kanatzidis, M. G. *J. Am. Chem. Soc.* **2005**, *127*, 9177.

(18) Kim, W.; Zide, J.; Gossard, A.; Klenov, D.; Stemmer, S.; Shakouri, A.; Majumdar, A. *Phys. Rev. Lett.* **2006**, *96*, 045901.